

Somatic mutations of the Parkinson's disease–associated gene *PARK2* in glioblastoma and other human malignancies

Selvaraju Veeriah^{1,10}, Barry S Taylor^{2,10}, Shasha Meng^{1,10}, Fang Fang¹, Emrullah Yilmaz¹, Igor Vivanco¹, Manickam Janakiraman¹, Nikolaus Schultz², Aphrothiti J Hanrahan¹, William Pao^{1,3}, Marc Ladanyi^{1,4}, Chris Sander², Adriana Heguy¹, Eric C Holland⁵, Philip B Paty⁶, Paul S Mischel⁷, Linda Liau⁷, Timothy F Cloughesy⁷, Ingo K Mellinger^{1,8}, David B Solit^{1,3} & Timothy A Chan^{1,9}

Mutation of the gene *PARK2*, which encodes an E3 ubiquitin ligase, is the most common cause of early-onset Parkinson's disease^{1–3}. In a search for multisite tumor suppressors, we identified *PARK2* as a frequently targeted gene on chromosome 6q25.2–q27 in cancer. Here we describe inactivating somatic mutations and frequent intragenic deletions of *PARK2* in human malignancies. The *PARK2* mutations in cancer occur in the same domains, and sometimes at the same residues, as the germline mutations causing familial Parkinson's disease. Cancer-specific mutations abrogate the growth-suppressive effects of the *PARK2* protein. *PARK2* mutations in cancer decrease *PARK2*'s E3 ligase activity, compromising its ability to ubiquitinate cyclin E and resulting in mitotic instability. These data strongly point to *PARK2* as a tumor suppressor on 6q25.2–q27. Thus, *PARK2*, a gene that causes neuronal dysfunction when mutated in the germline, may instead contribute to oncogenesis when altered in non-neuronal somatic cells.

mpg Parkinson's disease (PD) is the most common neurodegenerative movement disorder⁴. The familial, autosomal recessive form of PD is caused by germline mutations in the *PARK2* gene, which result in early-onset loss of dopaminergic neurons in the substantia nigra^{1–3,5}. *PARK2* is widely expressed in a variety of tissues, including the brain (in neurons and astrocytes), lung, colon and testes^{6–8}.

PARK2 associates with ubiquitin-conjugating enzymes, including UBCH7 and UBCH8, and is capable of promoting mono- and polyubiquitination of target proteins^{8–10}. In neuronal model systems, these activities can regulate proteasome-mediated degradation^{11,12}. *PARK2* can target a number of protein substrates, which have been identified primarily using systems focused on studying neuronal cytoprotection^{13–17}. Notably, *PARK2*-mediated degradation of cyclin E is important for preventing excitotoxicity in postmitotic neurons¹⁴. In neuronal model systems, *PARK2* mutations that cause juvenile PD

disrupt the ubiquitination activity of *PARK2* and the regulation of proteasome-mediated degradation^{8,9,12,14,18–21}. How *PARK2* loss leads to PD is not entirely clear.

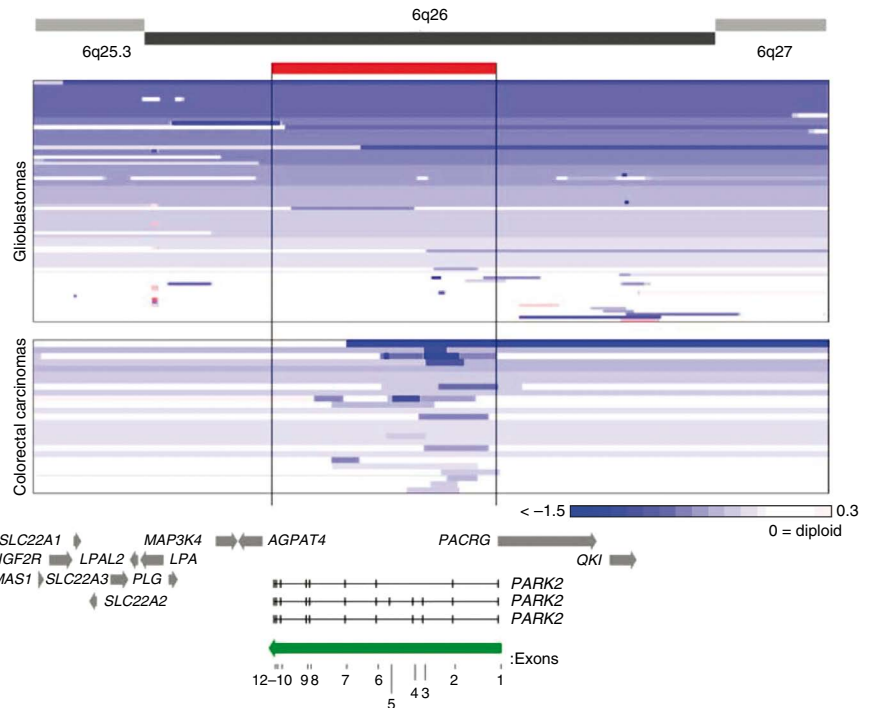
Chromosome 6q25.2–27 spans a large genomic region and undergoes frequent loss in a number of human cancers^{22–26}. *PARK2* is a potential candidate for a tumor suppressor gene at this locus, but intragenic mutations of this gene have not been reported^{25,27,28}. Furthermore, copy number loss within this region varies greatly in size from one tumor to another, and the identity of a common target of deletion remains unclear²⁹. *PARK2* maps near *FRA6E*, a common fragile site in the human genome, which displays complicated copy number variants. Like the locations of *FHIT* (3p14.2) and *WWOX* (16q23.3), this site is hypothesized to contain a tumor suppressor gene^{30,31}.

Here we present mutational and functional data that identify the ubiquitin E3 ligase *PARK2* as a chromosome 6q tumor suppressor in glioblastoma multiforme (GBM), colon cancer and lung cancer. To identify tumor suppressors that are targeted in multiple tumor types, we examined array comparative genomic hybridization (aCGH) results from 98 colon cancer samples and 216 GBM tumor samples. For colon cancer, analysis of loci that were recurrently deleted demonstrated a focal region on chromosome 6q (**Supplementary Fig. 1**). The GBM dataset is from the Cancer Genome Atlas (TCGA)²³. Copy number alterations (CNA) at the *PARK2* locus for both GBM and colon cancers are shown in **Figure 1**. As expected, we observed frequent heterozygous and homozygous loss of variable size on 6q in GBM (see Online Methods)²³. In GBM samples, 85% (53 out of 62) of samples with loss on 6q showed loss of the *PARK2* gene within the area of CNA. In colon cancer samples, 100% (24 out of 24) of samples with loss on 6q showed loss of *PARK2* within the CNA region. Loss of regions of various size encompassed *PARK2* and were found in a substantial portion of tumors (**Fig. 1, Table 1**). Notably, in both tumor types, intragenic homozygous deletions were found in the *PARK2* gene that removed exons but not any surrounding genes, thus pointing to *PARK2* as a targeted gene on

¹Human Oncology and Pathogenesis Program, ²Computational Biology Center, ³Department of Medicine, ⁴Department of Pathology, ⁵Department of Neurosurgery and ⁶Department of Surgery, Memorial Sloan-Kettering Cancer Center, New York, New York, USA. ⁷David Geffen School of Medicine, University of California, Los Angeles, California, USA. ⁸Department of Neurology and ⁹Department of Radiation Oncology, Memorial Sloan-Kettering Cancer Center, New York, New York, USA. ¹⁰These authors contributed equally to this work. Correspondence should be addressed to D.B.S. (solitd@mskcc.org) or T.A.C. (chant@mskcc.org).

Received 21 July; accepted 23 October; published online 29 November 2009; doi:10.1038/ng.491

Figure 1 Diversity of deletions at the *PARK2* locus in colon cancer and GBM. Array CGH segmentation map showing GBM (TCGA) and colon cancers (Memorial Sloan-Kettering Cancer Center) for the area surrounding *PARK2* on chromosome 6. Analysis and scores were calculated as previously described⁵⁷. Tumors are sorted by amount of loss at the *PARK2* locus for convenient viewing. Only tumors showing loss on 6q are shown. The color gradient depicts the extent of copy number loss. The position and boundaries of the *PARK2* gene (red bar) are indicated. *PARK2* direction and individual exons are labeled (green arrow). Surrounding genes are indicated with gray arrows.



chromosome 6q. Genomic loss in GBM samples tended to encompass broad regions including the *PARK2* gene, and intragenic microdeletions in *PARK2* occurred in 2.3% of samples (Fig. 1, Table 1). This pattern is also seen in lung cancer, which is thought to be associated with deletion of a putative tumor suppressor at 6q25–27. The identity of the gene of interest in this region is difficult to determine due to the variable nature of copy number loss in this tumor type²⁴. In contrast, the majority of the copy number loss on 6q25.2–q27 in our colon cancer samples occurred via focal events that affect *PARK2* but not surrounding genes (Fig. 1, bottom). Such focal losses occurred in approximately 25% of all colon cancer samples we examined (Table 1), robustly identifying the *PARK2* gene as the target of CNA. These results demonstrate the diversity of deletions at the *PARK2* locus. Focal deletions that target *PARK2* occur in both GBM and colon cancer, and *PARK2* constitutes a specifically targeted gene on 6q for both tumor types. It is well known that different tumor types have an intrinsic variation in the sizes of, and the tendency to undergo, this type of genetic abnormality, which may be dependent on chromatin state³². However, at least in the case of GBM, we cannot rule out the possibility that there exist other 6q tumor suppressors.

No somatic mutations in *PARK2* have been reported to date. To determine whether *PARK2* mutations are present in GBM and other human tumors, we sequenced all exons of the gene in 242 human cancers (Supplementary Table 1). Whenever a presumptive mutation was identified in a primary tumor, we verified that the change did not correspond to a known SNP and determined whether it was somatically acquired (that is, tumor specific) by examining the sequence of the gene in genomic DNA from normal tissue of the same individual. No study participant had a history of early-onset PD, nor did any carry germline PD-associated alleles. Using this strategy, we identified *PARK2* somatic mutations in human cancers for the first time, to our knowledge (Table 2, Supplementary Table 1 and Supplementary Fig. 2).

Figure 2 shows the distribution of our newly discovered mutations of *PARK2* in cancers (Fig. 2a, top diagram). The bottom diagram

shows the most common point mutations that cause early-onset PD. Notably, somatic *PARK2* mutations in cancer occur in the same domains as the germline PD mutations. In both cases, mutations cluster in the ubiquitin-like domain (UBL), the RING finger domain and the in-between RING fingers domain (IBR). Two residues, Arg42 and Arg275, are mutated both in colon cancer and GBM and in PD. However, the resultant amino acids differ between the somatic cancer mutations and the germline PD mutations. We have mapped several of the cancer-specific mutations that lie within domains whose structures have been solved (UBL and IBR)^{33,34}. The UBL domain is required for interactions with proteasomes and ligands. Disruption of Arg42 is predicted to disturb these interactions³³. Ile2 is located on the surface of the conserved β sheet of the UBL domain. The E344G mutation is located in the IBR domain, a region crucial for interaction with E2 and other members of the ubiquitination machinery^{35–37}. This mutation lies adjacent to the zinc-binding core and resides within a region predicted to be critical for proper ubiquitination (Fig. 2b)³⁴.

Examination of the copy number and mutation data (Fig. 1, Table 2) shows that although homozygous alterations do occur, most changes were heterozygous in nature. Thus, it may be that inactivation of a single copy of *PARK2* is sufficient to impart a clonal growth advantage during tumor development. It is interesting to note that, in the literature, there is well-described precedent for haploinsufficiency of another cyclin E–targeting E3 ligase—encoded by the tumor suppressor *FBXW7*, also known as *hCDC4* (ref. 38).

The molecular function of *PARK2* in neurons is a subject of considerable investigation, and it is still not clear how *PARK2* mutations cause PD. Less is known about the biological function of *PARK2* in human cancers. We first sought to determine if *PARK2* possesses growth-suppressive properties. *PARK2* protein expression was determined in several cell lines (Supplementary Fig. 3). We cloned wild-type (WT) *PARK2* cDNA and four *PARK2* mutants. Transfection of all cDNAs resulted in production of *PARK2* protein (Fig. 3a). To examine the functional consequences of reconstituting *PARK2* expression in cancer cells, we transfected WT *PARK2* into human cancer cell lines. *PARK2* potentially inhibited colony-forming activity in cell lines lacking *PARK2*

Table 1 Frequencies of *PARK2* copy number loss

Cancer type	Total samples with alterations	No. heterozygous loss	No. homozygous loss	Total samples
Glioblastoma	53 (24.5%)	48 (22.2%)	5 (2.3%)	216
Colon	24 (24.4%)	18 (18.4%)	6 (6.1%)	98
Total	77	66	11	314

Table 2 Somatic mutations of PARK2 in human cancers

Cancer type	Genomic position	Normal genotype	Tumor genotype	Amino acid change	Zygoty	Domain
Glioblastoma	161,889,928	GAG	GGG	E344G	Het	InterPro IPR002867 IBR domain
Glioblastoma	162,126,841	CGG	CAG	R275Q	Het	RING finger domain
Glioblastoma	162,542,170	ACG	GCG	T173A	Het	SH2-like domain
Glioblastoma	162,784,379	CGT	TGT	R42C	Het	InterPro IPR000626 ubiquitin domain
Glioblastoma	163,068,687	ATA	GTA	I2V	Het	InterPro IPR000626 ubiquitin domain
Glioblastoma	161,890,026	C	T	Eliminates 3' splice site (position 0)	Het	Exon 8
Glioblastoma cell line (T98G)	161,701,212	GAA	TAA	E395STOP	Het	Truncation
Lung	162,126,904	AAC	AGC	N254S	Het	RING finger domain
Lung	162,314,331	GAC	AAC	D243N	Het	RING finger domain
Lung	162,126,829	CAC	CCC	H279P	Het	RING finger domain
Lung	162,784,367	GCA	ACA	A46T	Hom	InterPro IPR000626 ubiquitin domain
Colon cell line	161,701,136	CGC	CAC	R420H	Het	RING finger domain
(DLD1 cell line; both alleles mut.)	161,727,847	GCC	GTC	A379V	Het	

Hom, homozygous; het, heterozygous; mut., mutated.

protein expression (Fig. 3b, Supplementary Fig. 4a) but not in cell lines that retained PARK2 expression (Fig. 3c, Supplementary Fig. 4b). We next sought to determine whether the cancer-specific mutations in PARK2 altered the protein's growth-suppressive properties. Expression of PARK2 with tumor-derived mutations resulted in substantially decreased colony-forming activity as compared to WT PARK2 (Fig. 3d, Supplementary Fig. 4c). Transfection of WT but not mutant PARK2 into cells from the DBTRG line resulted in a reduction in the rate of cell growth (Fig. 3e). WT PARK2 decreased tumor growth *in vivo*, a property that was reduced by the cancer-specific mutations (Fig. 3f). These data demonstrate that the PARK2 mutations in cancers have clear functional consequences.

What are the molecular mechanisms underlying PARK2 tumor suppression? PARK2 has previously been shown to be a ubiquitin E3 ligase that facilitates the ubiquitination of target proteins, leading to proteasome-mediated degradation^{8,13,39,40}. We first wanted to determine whether cancer-specific mutations in PARK2 altered its ubiquitin ligase activity. We used a well-established assay to measure the ubiquitination function of PARK2 mutants in cells^{8,11,41}. Cancer-specific mutations in PARK2 were found to substantially compromise the association of PARK2 with ubiquitinated target proteins in cancer cells (Fig. 4a). The mutations appeared to substantially decrease, but not completely abolish, the E3 ligase function. It is widely known

that cyclin E is a fundamental component of the cell cycle machinery and is encoded by an oncogene^{42–44}. We found that all PARK2 cancer mutations we analyzed resulted in a decreased ability of PARK2 to interact with cyclin E (Fig. 4b,c). Furthermore, the cancer-specific mutations compromised PARK2's ability to ubiquitinate cyclin E *in vitro* and degrade it (Fig. 4d). PARK2 mutations did not alter the protein's ability to regulate phosphorylation of c-Jun (Supplementary Fig. 5), another candidate effector of PARK2 function identified in neuronal systems^{19,45}. Thus, the cancer-specific mutations in PARK2 abrogate the protein's ability both to block tumor cell growth and to ubiquitinate cyclin E, establishing a mechanistic link for the loss-of-function mutations.

If PARK2 normally targets cyclin E for ubiquitination and degradation in cancer cells, then depletion of PARK2 should result in an increase of cyclin E levels. We knocked down PARK2 in four cancer cell lines that show PARK2 expression. In all cell lines examined, knockdown of PARK2 with two independent short interfering RNAs (siRNAs), but not with scrambled-sequence siRNAs, resulted in an accumulation of cyclin E levels (Fig. 4e). Thus, PARK2 mutation and inactivation disrupts the ability of PARK2 to ubiquitinate cyclin E.

Fluorescence-activated cell sorting analysis revealed that PARK2 knockdown increased the proportion of cells in the S and the G2-M phases (Fig. 4f). Immunofluorescence staining showed a significant increase in

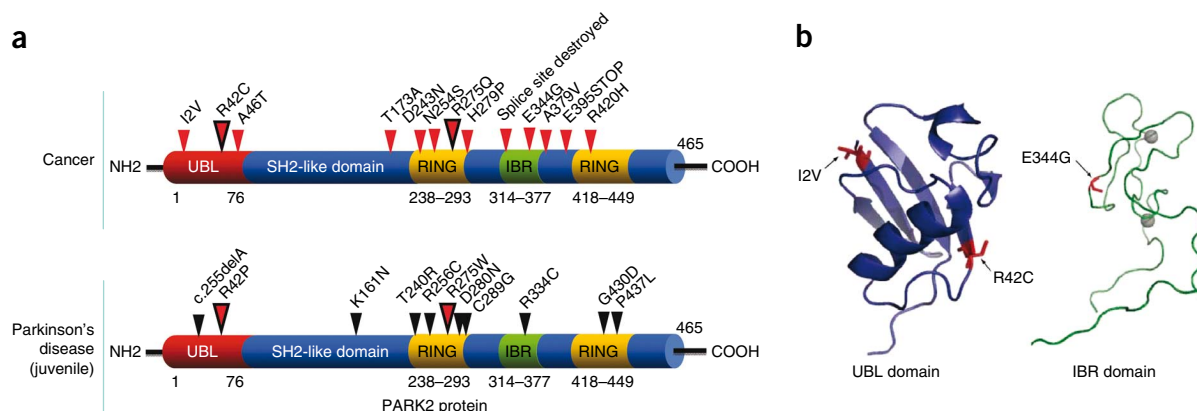


Figure 2 Somatic mutations of PARK2 in human cancers. (a) Summary of PARK2 mutations found in cancer (top) and early-onset Parkinson's disease (bottom). Small arrows show the location of mutations and corresponding amino acid changes. Larger dual-color arrows indicate amino acids that are affected in both cancer and PD; resultant amino acids are different. Mutations cluster in similar regions in both cancer and PD. (b) Structural analysis of cancer-specific mutations in the UBL (left) and IBR (right) domains. Ribbon diagram is shown (with alpha helices and beta sheets). Mutations are shown in red and labeled. Gray circles represent zinc atoms.

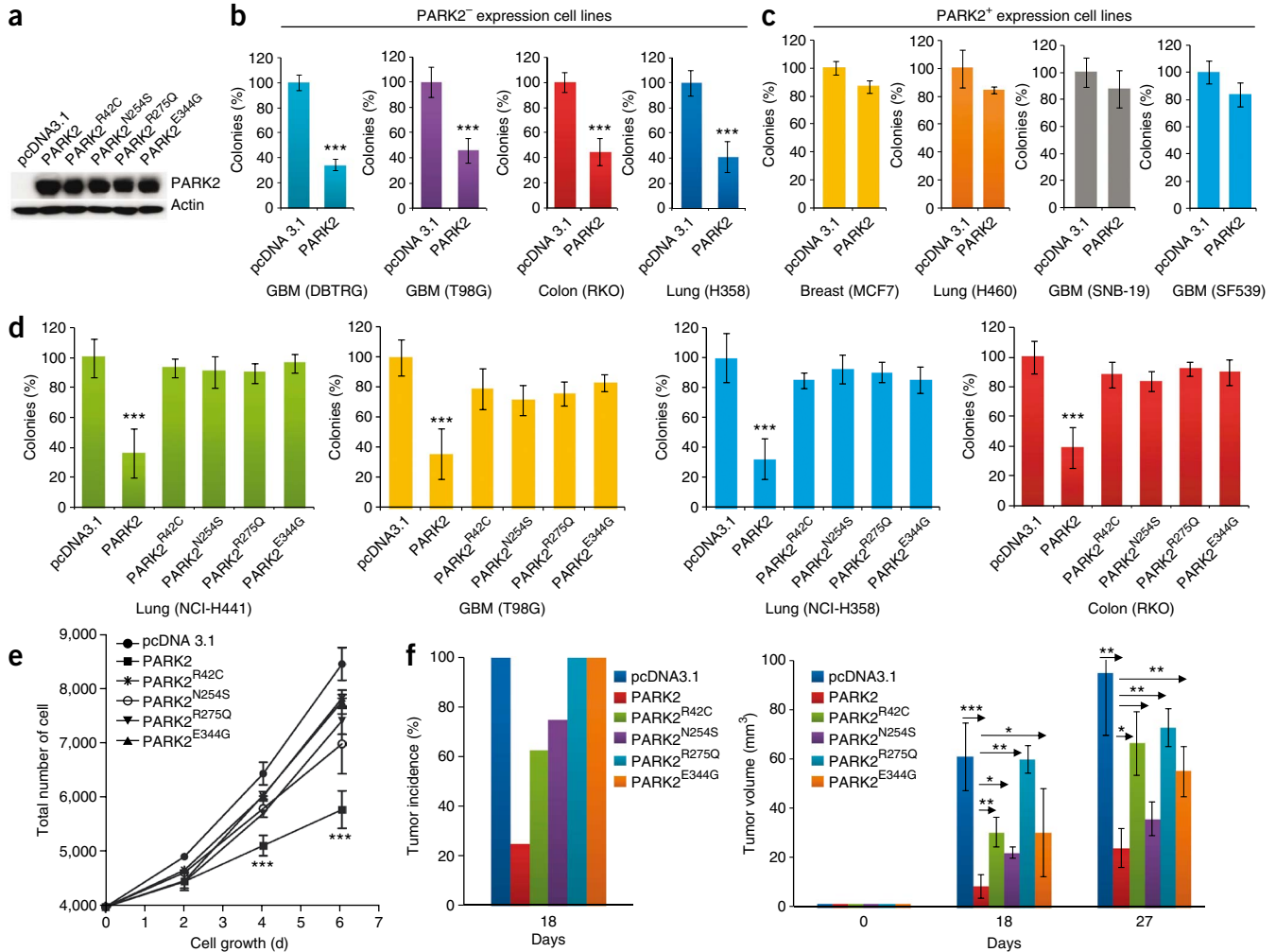


Figure 3 Functional analysis of somatic *PARK2* mutations in human cancer cell lines. **(a)** Protein blot showing expression of WT *PARK2* and *PARK2* with four cancer-specific mutations. Representative data for transfection into T98G are shown. pcDNA3.1, vector-only control. **(b)** Reconstitution of WT *PARK2* suppresses colony-forming ability of human cancer cells lacking *PARK2* expression. All assays performed in triplicate. Error bars, ± 1 s.d. $***P < 0.001$ (Student's *t*-test) in all cases. **(c)** Specificity of *PARK2* suppressive effects on colony formation. WT *PARK2* was transfected into *PARK2*-expressing cell lines. Suppressing effects on colony formation are minimal in *PARK2*⁺ lines. $P > 0.1$ (Student's *t*-test) for all experiments. Error bars, ± 1 s.d. **(d)** Tumor-derived mutations compromise the colony-forming ability of *PARK2* in cancer cells. WT or mutant *PARK2* was transfected into the cells indicated. All experiments performed in triplicate. $***P < 0.001$ (ANOVA) for all mutants. Error bars, ± 1 s.d. **(e)** Reconstitution of *PARK2* reduces growth rate in cancer cells. DBTRG cells were transfected with each of the constructs shown. All experiments were performed in triplicate. $***P < 0.0001$ (ANOVA) for WT *PARK2* compared to all others. Error bars, ± 1 s.d. **(f)** *PARK2* reconstitution results in decreased tumor growth *in vivo*. DBTRG glioma cells stably transfected with vector alone, WT *PARK2* and four *PARK2* mutants were injected as xenografts. Tumor incidence (left) and tumor size (right) are shown ($n = 16$). Days on x-axis refer to days following injection of cells into animals. All experiments were performed in duplicate. Arrows indicate comparisons made. $*P < 0.05$, $**P < 0.01$, $***P < 0.001$ (ANOVA). Error bars, ± 1 s.d.

the frequency of multipolar spindles and abnormal mitoses (Fig. 4g). Furthermore, *PARK2* knockdown cells showed a marked increase in nuclear atypia characterized by micronuclei. Notably, this is what one observes when cyclin E is overexpressed⁴⁶ or when FBXW7 (hCDC4), another protein that targets cyclin E for degradation, is inactivated^{47,48}. These data show that *PARK2* inactivation can lead to impaired mitosis.

The genetic and functional data we have presented demonstrate that the PD-associated gene *PARK2* is a bona fide tumor suppressor gene that is inactivated and mutated in GBM, colon cancer and lung cancer. Genetic loss or mutational inactivation of *PARK2* abrogates the ability of *PARK2* to promote ubiquitination and results in cyclin E dysregulation, which can promote tumor cell growth⁴⁹. Although the gene encoding cyclin E is an oncogene that has been strongly linked to tumorigenesis, we nevertheless cannot rule out the possibility that regulation of other targets

is important. In addition, our study reveals several important points. First, the finding of somatic mutations and high frequency intragenic copy-number loss provides the strongest evidence yet that *PARK2* is the (or at least one of the) 'long-sought' tumor suppressors on chromosome 6q. *PARK2* may be one of a select group of tumor suppressors inactivated in a wide range of human malignancies^{23,24,32,50}. Second, we determined that *PARK2* mutations in cancer can decrease the E3 ligase's ability to ubiquitinate cyclin E. Many human tumors have increased cyclin E levels⁴², but to date, the mechanisms underlying this increase are unclear. Our study suggests that *PARK2* can target cyclin E for ubiquitination, which, together with other factors such as FBXW7 (hCDC4), helps regulate cyclin E levels^{48,51,52}. Because *PARK2* is mutated in both PD and cancer, it is tempting to hypothesize that alterations of this gene may result in very different phenotypes depending on cellular context (Supplementary Fig. 6).

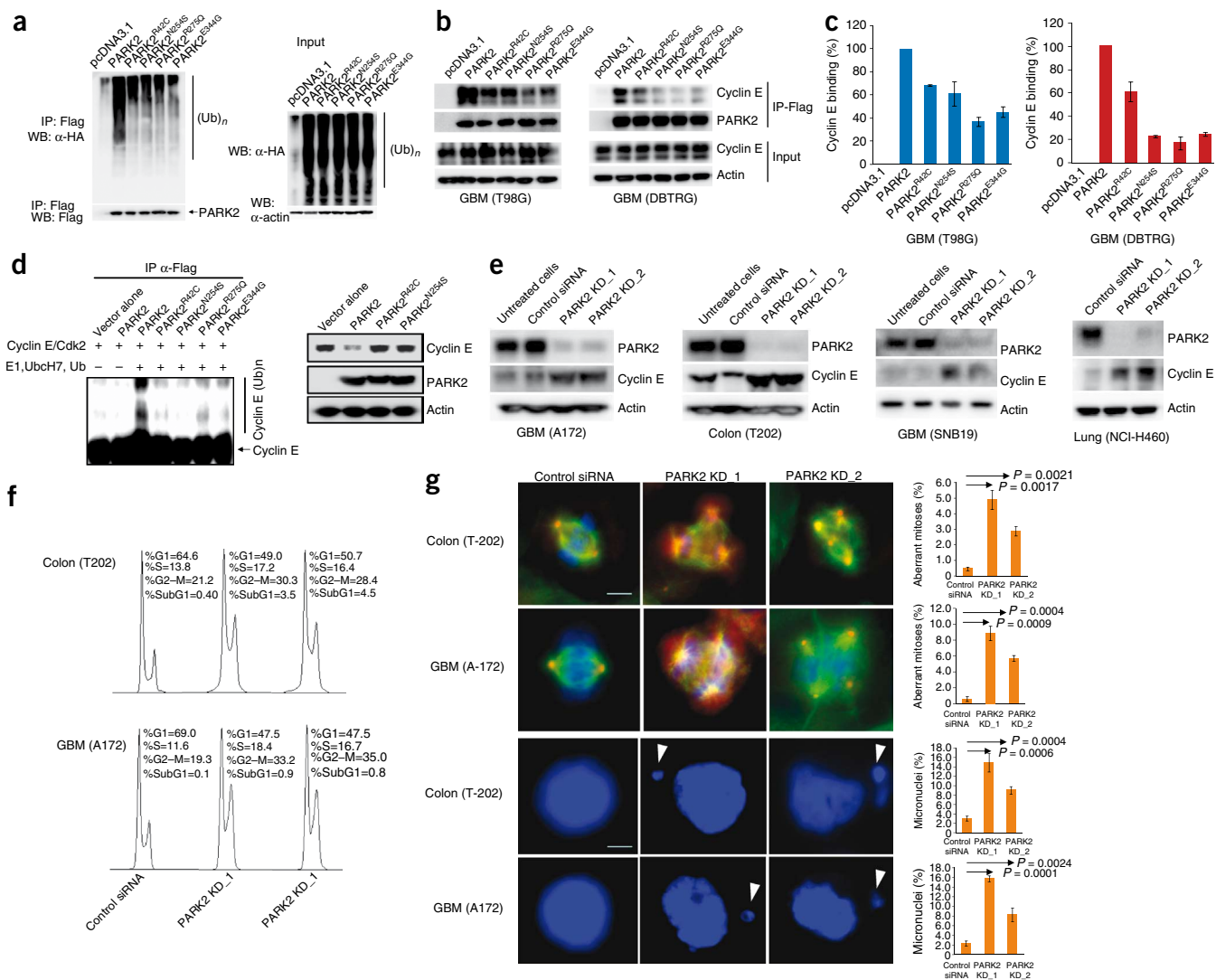


Figure 4 *PARK2* cancer-specific mutations compromise ubiquitination activity. (a) Tumor-derived mutations disrupt *PARK2*-mediated ubiquitination in cancer cells. T98G cells were transfected with hemagglutinin-ubiquitin (HA-Ub), vector only (pcDNA3.1), WT *PARK2* (Flag-tagged) or one of four mutant *PARK2* cDNAs (Flag-tagged). Assay was performed as previously described⁵. (b) Cancer-derived mutations of *PARK2* decrease association with cyclin E. Indicated cells were treated as above, immunoprecipitated with Flag and detected by protein blot. (c) Quantitation of cyclin E binding efficiency by densitometry. Representative plots shown. For each mutant versus WT, $P < 0.05$ (Student's *t*-test). Error bars, ± 1 s.d. (d) Protein blot showing cancer-derived mutations that compromise *PARK2*-mediated cyclin E ubiquitination *in vitro* (left). Expression of WT *PARK2* but not mutant *PARK2* decreases cyclin E levels (right). (e) Knockdown of *PARK2* results in increased cyclin E levels. Cells indicated were transfected with *PARK2* siRNAs or scrambled siRNA controls and protein blots were performed. (f) Flow cytometry analysis of the indicated cells following *PARK2* knockdown. Experiments were performed in triplicate. Representative results are shown. (g) Knockdown of *PARK2* results in multipolar spindles and increased frequency of abnormal mitoses (top two rows) and the development of micronuclei (bottom two rows, white arrows). Examples for indicated cells shown using siRNAs targeting *PARK2* and scrambled siRNA controls. Red, γ -tubulin; green, α -tubulin. Graphs show quantitation of experiments. Black arrows indicate comparisons made and corresponding *P* values (Student's *t*-test). White scale bar for top two rows, 15 μ m; bottom two rows, 5 μ m. Error bars, ± 1 s.d.

The finding of somatic mutations of *PARK2*, a PD-causing gene, in cancer is noteworthy from a pathophysiologic standpoint. It seems that inactivation of certain genes, such as *PARK2*, results in distinct physiological outcomes depending on cellular context. Indeed, the *PTEN* and *ATM* genes function as tumor suppressors, but their inactivation also leads to neuronal loss when the mutations are in the germline^{53,54}. Unlike in these two cases, *PARK2* germline mutation gives rise to a neurological disease but not also to a cancer predisposition syndrome. It is possible that *PARK2* function may result in biological outcomes that are very different depending on whether the affected cell is a neuron or a dividing cell such as an astrocyte or epithelial cell; this seems more true for *PARK2* than for *PTEN* or

ATM. Notably, cohorts of individuals with PD do reveal a small but significant increase in the risk of malignancies such as brain and lung cancers^{55,56}. We believe our study has wide implications for understanding oncogenesis for a number of tumor types.

METHODS

Methods and any associated references are available in the online version of the paper at <http://www.nature.com/naturegenetics/>.

Accession numbers. Colon cancer datasets are deposited in the Gene Expression Omnibus via accession number GSE18638. All GBM datasets are publicly available at <http://cancergenome.nih.gov/>.

Note: Supplementary information is available on the Nature Genetics website.

ACKNOWLEDGMENTS

We thank J. Wongvipat, K. Huberman, I. Dolgalev and S. Thomas for exceptional technical expertise. We thank R. Levine for helpful discussions and comments. B.S.T. is the David H. Koch Fellow in cancer genomics. This work was supported in part by The Brain Tumors Funders' Collaborative Fund (I.K.M.), The Cancer Genome Atlas Project (N.S., C.S.), the Flight Attendants Medical Research Institute (T.A.C.), the Louis Gerstner Foundation (T.A.C.), the Memorial Sloan-Kettering Society (T.A.C.), the Elsa U. Pardee Foundation (T.A.C.) and the Doris Duke Charitable Foundation (T.A.C.).

AUTHOR CONTRIBUTIONS

T.A.C. and S.V. designed the experiments. S.V., S.M., F.F., E.Y. and M.J. performed the experiments. S.V., B.S.T., N.S., C.S. and T.A.C. analyzed the data. W.P., M.L., E.C.H., I.V., P.B.P., L.L., P.S.M., A.H., T.F.C., A.J.H., I.K.M. and D.B.S. contributed new reagents and analytic tools. T.A.C. and S.V. wrote the paper.

Published online at <http://www.nature.com/naturegenetics/>.

Reprints and permissions information is available online at <http://npg.nature.com/reprintsandpermissions/>.

- Kitada, T. *et al.* Mutations in the parkin gene cause autosomal recessive juvenile parkinsonism. *Nature* **392**, 605–608 (1998).
- Lücking, C.B. *et al.* Association between early-onset Parkinson's disease and mutations in the parkin gene. *N. Engl. J. Med.* **342**, 1560–1567 (2000).
- Fearnley, J.M. & Lees, A.J. Ageing and Parkinson's disease: substantia nigra regional selectivity. *Brain* **114**, 2283–2301 (1991).
- Samii, A., Nutt, J.G. & Ransom, B.R. Parkinson's disease. *Lancet* **363**, 1783–1793 (2004).
- Abbas, N. *et al.* A wide variety of mutations in the parkin gene are responsible for autosomal recessive parkinsonism in Europe. French Parkinson's Disease Genetics Study Group and the European Consortium on Genetic Susceptibility in Parkinson's Disease. *Hum. Mol. Genet.* **8**, 567–574 (1999).
- Ledesma, M.D. *et al.* Astrocytic but not neuronal increased expression and redistribution of parkin during unfolded protein stress. *J. Neurochem.* **83**, 1431–1440 (2002).
- Kitada, T. *et al.* Molecular cloning, gene expression, and identification of a splicing variant of the mouse parkin gene. *Mamm. Genome* **11**, 417–421 (2000).
- Shimura, H. *et al.* Familial Parkinson disease gene product, parkin, is a ubiquitin-protein ligase. *Nat. Genet.* **25**, 302–305 (2000).
- Hampe, C. *et al.* Biochemical analysis of Parkinson's disease-causing variants of Parkin, an E3 ubiquitin-protein ligase with monoubiquitylation capacity. *Hum. Mol. Genet.* **15**, 2059–2075 (2006).
- Corti, O. *et al.* Parkinson's disease: from causes to mechanisms. *C. R. Biol.* **328**, 131–142 (2005).
- Shimura, H. *et al.* Ubiquitination of a new form of alpha-synuclein by parkin from human brain: implications for Parkinson's disease. *Science* **293**, 263–269 (2001).
- Sriram, S.R. *et al.* Familial-associated mutations differentially disrupt the solubility, localization, binding and ubiquitination properties of parkin. *Hum. Mol. Genet.* **14**, 2571–2586 (2005).
- Corti, O. *et al.* The p38 subunit of the aminoacyl-tRNA synthetase complex is a Parkin substrate: linking protein biosynthesis and neurodegeneration. *Hum. Mol. Genet.* **12**, 1427–1437 (2003).
- Staropoli, J.F. *et al.* Parkin is a component of an SCF-like ubiquitin ligase complex and protects postmitotic neurons from kainate excitotoxicity. *Neuron* **37**, 735–749 (2003).
- Moore, D.J. *et al.* Parkin mediates the degradation-independent ubiquitination of Hsp70. *J. Neurochem.* **105**, 1806–1819 (2008).
- Smith, W.W. *et al.* Leucine-rich repeat kinase 2 (LRRK2) interacts with parkin, and mutant LRRK2 induces neuronal degeneration. *Proc. Natl. Acad. Sci. USA* **102**, 18676–18681 (2005).
- Imai, Y. *et al.* CHIP is associated with Parkin a gene responsible for familial Parkinson's disease, and enhances its ubiquitin ligase activity. *Mol. Cell* **10**, 55–67 (2002).
- Hasegawa, T. *et al.* Parkin protects against tyrosinase-mediated dopamine neurotoxicity by suppressing stress-activated protein kinase pathways. *J. Neurochem.* **105**, 1700–1715 (2008).
- Liu, M. *et al.* Parkin regulates Eg5 expression by Hsp70 ubiquitination-dependent inactivation of c-Jun NH2-terminal kinase. *J. Biol. Chem.* **283**, 35783–35788 (2008).
- Imai, Y., Soda, M. & Takahashi, R. Parkin suppresses unfolded protein stress-induced cell death through its E3 ubiquitin-protein ligase activity. *J. Biol. Chem.* **275**, 35661–35664 (2000).
- Zhang, Y. *et al.* Parkin functions as an E2-dependent ubiquitin-protein ligase and promotes the degradation of the synaptic vesicle-associated protein, CDCrel-1. *Proc. Natl. Acad. Sci. USA* **97**, 13354–13359 (2000).
- Parsons, D.W. *et al.* An integrated genomic analysis of human glioblastoma multiforme. *Science* **321**, 1807–1812 (2008).
- Cancer Genome Atlas Research Network. Comprehensive genomic characterization defines human glioblastoma genes and core pathways. *Nature* **455**, 1061–1068 (2008).
- Weir, B.A. *et al.* Characterizing the cancer genome in lung adenocarcinoma. *Nature* **450**, 893–898 (2007).
- Cesari, R. *et al.* Parkin, a gene implicated in autosomal recessive juvenile parkinsonism, is a candidate tumor suppressor gene on chromosome 6q25-q27. *Proc. Natl. Acad. Sci. USA* **100**, 5956–5961 (2003).
- Toma, M.I. *et al.* Loss of heterozygosity and copy number abnormality in clear cell renal cell carcinoma discovered by high-density Affymetrix 10K single nucleotide polymorphism mapping array. *Neoplasia* **10**, 634–642 (2008).
- Denison, S.R. *et al.* Alterations in the common fragile site gene Parkin in ovarian and other cancers. *Oncogene* **22**, 8370–8378 (2003).
- Wang, F. *et al.* Parkin gene alterations in hepatocellular carcinoma. *Genes Chromosom. Cancer* **40**, 85–96 (2004).
- Yin, D. *et al.* High-resolution genomic copy number profiling of glioblastoma multiforme by single nucleotide polymorphism DNA microarray. *Mol. Cancer Res.* **7**, 665–677 (2009).
- Ohta, M. *et al.* The FHIT gene, spanning the chromosome 3p14.2 fragile site and renal carcinoma-associated t(3;8) breakpoint, is abnormal in digestive tract cancers. *Cell* **84**, 587–597 (1996).
- Sozzi, G. *et al.* The FHIT gene 3p14.2 is abnormal in lung cancer. *Cell* **85**, 17–26 (1996).
- Cox, C. *et al.* A survey of homozygous deletions in human cancer genomes. *Proc. Natl. Acad. Sci. USA* **102**, 4542–4547 (2005).
- Sakata, E. *et al.* Parkin binds the Rpn10 subunit of 26S proteasomes through its ubiquitin-like domain. *EMBO Rep.* **4**, 301–306 (2003).
- Beasley, S.A., Hristova, V.A. & Shaw, G.S. Structure of the Parkin in-between-ring domain provides insights for E3-ligase dysfunction in autosomal recessive Parkinson's disease. *Proc. Natl. Acad. Sci. USA* **104**, 3095–3100 (2007).
- Dächsel, J.C. *et al.* Parkin interacts with the proteasome subunit alpha4. *FEBS Lett.* **579**, 3913–3919 (2005).
- Rankin, C.A., Joazeiro, C.A., Floor, E. & Hunter, T. E3 ubiquitin-protein ligase activity of Parkin is dependent on cooperative interaction of RING finger (TRIAD) elements. *J. Biomed. Sci.* **8**, 421–429 (2001).
- Martinez-Noel, G., Müller, U. & Harbers, K. Identification of molecular determinants required for interaction of ubiquitin-conjugating enzymes and RING finger proteins. *Eur. J. Biochem.* **268**, 5912–5919 (2001).
- Mao, J.H. *et al.* Fbxw7/Cdc4 is a p53-dependent, haploinsufficient tumour suppressor gene. *Nature* **432**, 775–779 (2004).
- Betarbet, R., Sherer, T.B. & Greenamyre, J.T. Ubiquitin-proteasome system and Parkinson's diseases. *Exp. Neurol.* **191**(Suppl. 1), S17–S27 (2005).
- Dohm, C.P., Kermer, P. & Bahr, M. Aggregopathy in neurodegenerative diseases: mechanisms and therapeutic implication. *Neurodegener. Dis.* **5**, 321–338 (2008).
- Schlossmacher, M.G. & Shimura, H. Parkinson's disease: assays for the ubiquitin ligase activity of neural Parkin. *Methods Mol. Biol.* **301**, 351–369 (2005).
- Donnellan, R. & Chetty, R. Cyclin E in human cancers. *FASEB J.* **13**, 773–780 (1999).
- Courjal, F. *et al.* Cyclin gene amplification and overexpression in breast and ovarian cancers: evidence for the selection of cyclin D1 in breast and cyclin E in ovarian tumors. *Int. J. Cancer* **69**, 247–253 (1996).
- Kitagawa, K., Kotake, Y. & Kitagawa, M. Ubiquitin-mediated control of oncogene and tumor suppressor gene products. *Cancer Sci.* **100**, 1374–1381 (2009).
- Um, J.W. *et al.* Molecular interaction between parkin and PINK1 in mammalian neuronal cells. *Mol. Cell. Neurosci.* **40**, 421–432 (2009).
- Keck, J.M. *et al.* Cyclin E overexpression impairs progression through mitosis by inhibiting APC(Cdh1). *J. Cell Biol.* **178**, 371–385 (2007).
- Rajagopalan, H. *et al.* Inactivation of hCDC4 can cause chromosomal instability. *Nature* **428**, 77–81 (2004).
- Ekholm-Reed, S. *et al.* Mutation of hCDC4 leads to cell cycle deregulation of cyclin E in cancer. *Cancer Res.* **64**, 795–800 (2004); erratum **64**, 2939 (2004).
- Spruck, C.H., Won, K.A. & Reed, S.I. Deregulated cyclin E induces chromosome instability. *Nature* **401**, 297–300 (1999).
- Mhawech-Fauceglia, P. *et al.* Array-comparative genomic hybridization analysis of primary endometrial and ovarian high-grade neuroendocrine carcinoma associated with adenocarcinoma: mystery resolved? *Int. J. Gynecol. Pathol.* **27**, 539–546 (2008).
- Sangfelt, O. *et al.* Both SCF(Cdc4a) and SCF(Cdc4y) are required for cyclin E turnover in cell lines that do not overexpress cyclin E. *Cell Cycle* **7**, 1075–1082 (2008).
- Strohmaier, H. *et al.* Human F-box protein hCdc4 targets cyclin E for proteolysis and is mutated in a breast cancer cell line. *Nature* **413**, 316–322 (2001).
- Eng, C. PTEN: one gene, many syndromes. *Hum. Mutat.* **22**, 183–198 (2003).
- Shiloh, Y. & Rotman, G. Ataxia-telangiectasia and the ATM gene: linking neurodegeneration, immunodeficiency, and cancer to cell cycle checkpoints. *J. Clin. Immunol.* **16**, 254–260 (1996).
- Olsen, J.H. *et al.* Atypical cancer pattern in patients with Parkinson's disease. *Br. J. Cancer* **92**, 201–205 (2005).
- Møller, H., Møllekjær, L., McLaughlin, J.K. & Olsen, J.H. Occurrence of different cancers in patients with Parkinson's disease. *Br. Med. J.* **310**, 1500–1501 (1995).
- Taylor, B.S. *et al.* Functional copy-number alterations in cancer. *PLoS One* **3**, e3179 (2008).

ONLINE METHODS

Tumor samples, array CGH analysis and bioinformatics. Colon tumor samples ($n = 98$) from the Memorial Sloan-Kettering Cancer Center were obtained following participant consent and with institutional review board approval (**Supplementary Note**). Source DNAs were extracted from primary tumors for the aCGH study. The GBMs ($n = 216$) in the aCGH study were part of the TCGA initiative (4/14/2008 data freeze) (see URL section). aCGH was performed using the Agilent 244K microarray according to the manufacturer's instructions (Agilent Technologies). In our examination of both the colon cancer and GBM datasets, analysis of data for the CNAs observed was performed using the RAE method. The status of genomic loss at the *PARK2* locus in colon cancer samples was assigned as either likely heterozygous loss ($D_0 \geq 0.9$) or homozygous deletion ($D_0 \geq 0.9$ and $D_1 \geq 0.5$), and in GBM as previously described per the multi-component model in RAE^{23,57}. Cell lines sequenced were T98G, DBTRG, RKO, H441 and H358.

PCR amplification and sequencing. Exonic regions for the *PARK2* gene (NCBI Human Genome Build 36.1) were broken into 16 amplicons of 500 bp or less, and specific primers were designed using Primer3. Primers are listed in **Supplementary Table 2**. Standard M13 tails were added to the primers to facilitate Sanger sequencing. PCR reactions were carried out in 384-well plates in a Duncan DT-24 water bath thermal cycler with 10 ng of whole-genome amplified DNA (REPLI-g Midi, Qiagen) as a template, using a touchdown PCR protocol with **KAPA Fast HotStart (Kapa Biosystems)**. The touchdown PCR method consisted of: 1 cycle of 95 °C for 5 min; 3 cycles of 95 °C for 30 s, 64 °C for 15 s, 72 °C for 30 s; 3 cycles of 95 °C for 30 s, 62 °C for 15 s, 72 °C for 30 s; 3 cycles of 95 °C for 30 s, 60 °C for 15 s, 72 °C for 30 s; 37 cycles of 95 °C for 30 s, 58 °C for 15 s, 72 °C for 30 s; 1 cycle of 70 °C for 5 min. Templates were purified using AMPure (Agencourt Biosciences). The purified PCR reactions were split into two and sequenced bidirectionally with M13 forward and reverse primer and the Big Dye Terminator Kit v.3.1 (Applied Biosystems) at Agencourt Biosciences. Dye terminators were removed using the CleanSEQ kit (Agencourt Biosciences), and sequence reactions were run on ABI PRISM 3730xl sequencing apparatus (Applied Biosystems).

Mutation detection. Passing reads were assembled against the *PARK2* reference sequence, which contains all coding exons in *PARK2* including those 5 kb upstream and downstream of the gene, using command line Consed 16.0 (ref. 58). Assemblies were passed on to Polyphred 6.02b⁵⁹, which generated a list of putative candidate mutations, and to Polyscan 3.0 (ref. 60), which generated a second list of putative mutations. The lists were merged together into a combined report, and the putative mutation calls were normalized to '+' genomic coordinates and annotated using the genomic mutation consequence calculator⁶¹. The resulting list of annotated putative mutations was loaded into a Postgres database along with select assembly details for each mutation call (assembly position, coverage and methods supporting mutation call). To reduce the number of false positives generated by the mutation detection software packages, only point mutations that are supported by at least one bidirectional read pair and at least one sample mutation called by Polyphred were considered, and only the putative mutations that are annotated as having nonsynonymous coding effects, occur within 11 bp of an exon boundary, or have a conservation score >0.699 (see URL section) were included in the final candidate list. Indels were manually reviewed and included in the candidate list if found to hit an exon. All putative mutations were confirmed by a second PCR and sequencing reaction in parallel with amplification and sequencing of matched normal tissue DNA.

Cell culture. All cell lines were obtained from American Type Tissue Culture and cultured using the recommended media (Invitrogen) + 10% FBS (Invitrogen) and penicillin plus streptomycin at 37 °C in 5% CO₂. HEK 293T cells were cultured in Dulbecco's modified eagle's medium (DMEM) + 10% FBS (Invitrogen). Expression of *PARK2* was accomplished by cloning the

gene into the vector pcDNA 3.1 with a Flag tag (Invitrogen). Transfection was performed using Lipofectamine reagent according to the manufacturer's protocol (Invitrogen). Selection was performed using G418 or hygromycin. Cells used in colony formation assays were stained with crystal violet. Growth curve assays were quantified by manual counting with a Motic inverted microscope. All experiments were performed in triplicate.

Protein blot, immunoprecipitation and immunostaining. Protein blot analysis was performed using standard methods. Antibody against the Flag epitope, the hemagglutinin tag and beta-actin were obtained from Sigma. *PARK2* and cyclin E1 antibodies were obtained from Cell Signaling. Immunoprecipitation was performed using the Flag immunoprecipitation kit (Sigma). *In vivo* ubiquitination assay was performed as previously described⁸. The *in vitro* *PARK2* ubiquitination assay was performed using the Parkin ubiquitination kit (Boston Biochem) per the manufacturer's protocol. Immunostaining was performed with antibodies to α -tubulin and γ -tubulin as previously described⁴⁷. Staining for atypical nuclei and micronuclei was performed as previously described 48 h after siRNA transfection⁴⁷.

Knockdown of *PARK2*. *PARK2* siRNAs were obtained from Invitrogen. *PARK2* targeted sequences are listed in **Supplementary Table 2**. For siRNA knockdown of *PARK2*, cells were transfected using Lipofectamine RNAiMAX system (Invitrogen).

Retrovirus production. For retrovirus production, WT *PARK2* and mutants were cloned into the vector pQCXIP (Clontech). HEK 293T cells were seeded in 10-cm-diameter dishes. The HEK 293T packaging cells (at 30–50% confluency) were co-transfected using Lipofectamine (Invitrogen) with pE-ampho vector (Takara Bio) and pQCXIP-*PARK2*. Retroviral particles were collected, filtered through the 0.45- μ m syringe filter and used in the presence of polybrene (8 μ g/ml final concentration) to infect cells for 12 h.

Site-directed mutagenesis. Mutations identified were engineered into pcDNA3.1-*PARK2* using the QuikChange II XL kit (Stratagene). All changes were verified by Sanger sequencing.

Flow cytometry. Cells were trypsinized, fixed and stained using the standard propidium iodide method 48 h after transfection. Cell cycle analysis was performed on stained cells using a MoFlo cell sorter (Cytomation).

Mouse xenograft studies. 1×10^6 cells were suspended in 50% Matrigel and injected into the flanks of severe combined immunodeficiency mice. Growth was followed over time by taking caliper measurements. Eight mice were injected and 16 tumors were assessed for each condition.

Statistical analysis. Two-tailed Student's *t*-test analysis was performed using GraphPad Prism software.

URLs. TCGA initiative, <http://cancergenome.nih.gov/index.asp>; Primer3, <http://frodo.wi.mit.edu/primer3/>; Postgres, <http://www.postgresql.org/>; 17-way Cons Track Settings, <http://genome.ucsc.edu/cgi-bin/hgTrackUi?hgssid=108554407&g=multiz17way>; GraphPad Prism, <http://www.graphpad.com/prism/Prism.htm>.

58. Gordon, D., Abajian, C. & Green, P. Consed: a graphical tool for sequence finishing. *Genome Res.* **8**, 195–202 (1998).
59. Nickerson, D.A., Tobe, V.O. & Taylor, S.L. PolyPhred: automating the detection and genotyping of single nucleotide substitutions using fluorescence-based resequencing. *Nucleic Acids Res.* **25**, 2745–2751 (1997).
60. Chen, K. *et al.* PolyScan: an automatic indel and SNP detection approach to the analysis of human resequencing data. *Genome Res.* **17**, 659–666 (2007).
61. Major, J.E. Genomic mutation consequence calculator. *Bioinformatics* **23**, 3091–3092 (2007).